WDS'24 Proceedings of Contributed Papers — Physics, 82–88, 2024. ISBN 978-80-7378-520-8 © MATFYZPRESS

Development of Magnetic Field Diagnostics for Fusion Reactors

M. Ivánek,[1,2] I. Ďuran,[2] S. Entler,[2] A. Torres,[2] P. Sládek,[2] M. Šimonovský,[3] P. Turjanica,[4,2] and J. Řeboun[4,2]

[1] Charles University, Faculty of Mathematics and Physics, Prague, Czech Republic.
[2] Institute of Plasma Physics of the Czech Academy of Sciences, Prague, Czech Republic.
[3] ELCERAM a.s., Hradec Kralove, Czech Republic.
[4] University of West Bohemia, Pilsen, Czech Republic.

Abstract. Magnetic diagnostics play a crucial role in determining key parameters of tokamak plasmas, such as plasma position and shape. Traditional methods for measuring magnetic fields during tokamak discharges rely on inductive sensors, such as pick-up coils. While these sensors are adequate for tokamaks with relatively short pulses and limited radiation levels, fusion reactors with long pulse lengths and high radiation environments require the use of steady-state magnetic field sensors, such as Hall sensors. In this paper, the principles behind magnetic field measurement in the fusion plasma environment will be reviewed. The performance and drawbacks of pick-up coils will be described, and advancements in Hall sensor development for fusion reactors will be outlined. The challenges associated with the utilisation of Hall sensors in such environments will be addressed, including the necessary techniques such as synchronous detection and current spinning. Finally, the potential for data fusion of inductive and Hall sensors using the Kalman filter algorithm to enhance measurement accuracy will be discussed.

Introduction

Thermonuclear fusion is a process of fusing lighter nuclei into heavier ones at high temperatures producing energy. A common characteristic among fusion reactions is the fact that they can only happen at a reasonable rate at temperatures in the order of 10^8 °C and above. This leads to the problem of containing the hot fuel and preventing it from coming into contact with any structures of a potential fusion reactor. One of the solutions to this question is a tokamak which is a device that contains hot plasma using magnetic fields. It is thus important to be able to measure said magnetic field accurately as it is an integral part of the operation of a tokamak-based fusion reactor.

One of the methods for measuring the magnetic field is by inductive sensors. Their most defining characteristic is that their output signal is proportional to the derivative of the measured magnetic field. This means that they possess a low sensitivity to fields with low frequency and that because of the required integration of their output signal, they are prone to low-frequency error voltages. Despite this fact the use of inductive sensors is common on all magnetic confinement fusion devices and their use is expected on future magnetic confinement devices as well.

As a complement to inductive sensors radiation resistant Hall sensors are developed. Commercially available Hall sensors are widely used in many areas of everyday life such as in automotive where they serve as sensors of position or rotation. However, these are mostly based on semiconductor materials and thus possess a relatively low maximum operating temperature of around 150 °C and their radiation resistance is low as well rendering them unsuitable for use in environments produced by fusion reactors [*Ďuran et al.*, 2006]. Therefore Hall sensors with metallic sensitive layers are being developed at the Institute of Plasma Physics of Czech Academy of Sciences. These sensors offer a higher maximum operating temperature from 250 °C and above and are also able to withstand significant radiation fluence [*Ďuran et al.*, 2017; *Entler et al.*, 2019, 2021a, 2023]. However, due to the metallic sensitive layers, these sensors have a significantly lower sensitivity compared to the commercially available ones. This leads to the employment of various signal conditioning methods to isolate the low-level signal that metallic Hall sensors produce. This signal processing limits the bandwidth of the sensors and makes them only viable as steady-state diagnostics as the cut-off frequency of the sensors with the signal conditioning employed is only in the order of few tens of Hz.

Having one type of sensor performing well at low frequencies and the other type perform well at higher frequencies gives rise to the question of whether it is possible to combine those sensors in such a way that compensates the drawbacks of the individual sensors. To combine the inductive and Hall sensors, the Kalman filtering algorithm is explored.

In this paper, the principles behind magnetic field measurement in the fusion plasma environment will be

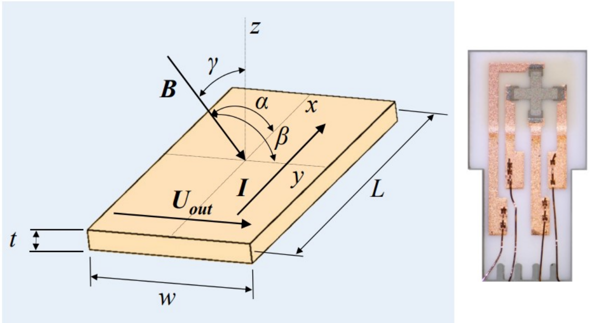

Figure 1. Schematic of a sensor based on Hall effect. Available from *Entler et al.* [2017b] (left). Hall sensor with an antimony sensing layer, W/Ti diffusion barriers and Al_2O_3 passivation layer developed at IPP CAS (right).

reviewed. The performance and drawbacks of pick-up coils will be described, and advancements in Hall sensor development for fusion reactors will be outlined. The challenges associated with the utilisation of Hall sensors in such environments will be addressed, including the necessary techniques such as synchronous detection and current spinning. Finally, the potential for data fusion of inductive and Hall sensors using the Kalman filter algorithm to enhance measurement accuracy will be discussed.

Magnetic diagnostics

Since magnetic field is an integral part of a tokamak an accurate system of magnetic diagnostics is an operational requirement for any such device. The term magnetic diagnostics, apart from the sensors of the magnetic field, include diamagnetic loops, flux loops and Rogowski coils. In this contribution inductive and Hall sensors will be investigated.

Inductive sensors

Sensors based on electromagnetic induction are a common way to measure magnetic fields. Their defining characteristic is their output signal being proportional to the time derivative of the measured magnetic field. The proportionality coefficient is the effective area A_c of the sensor as described in equation (1)

$$U_\mathrm{out} = A_\mathrm{c}\frac{\partial B}{\partial t}. \tag{1}$$

This results in their low sensitivity to low-frequency magnetic fields. Moreover, low-frequency error voltages arising from sources other than the measured magnetic field cause signal drifting after the subsequent integration of the signal. Since such error voltages may arise due to temperature gradients caused by inhomogeneous radiation heating they are difficult to predict and thus almost impossible to dispose of in real time. The requirement accepted for ITER is to suppress the amount of drift over the duration of the discharge. The limit of inductive sensor drift for ITER is according to *Batista et al.* [2018] 500 µVs/hour.

Hall sensors

A method complementary to inductive sensors is Hall sensors. They are widely used in many areas of everyday life. Such as in robotics or automotive where they can be used as sensors of position or rotation. They are based on the Hall effect which occurs when, as depicted in Figure 1(left), a conductive or semi-conductive plate is biased by a current I and placed in an external magnetic field. In such case, Hall voltage U_H perpendicular to the biasing current is observed.

This effect occurs due to the Lorentz force acting upon the free charge carriers in the conductive plate.Its influence is in the direction perpendicular to both the carriers' velocity and the applied magnetic field. The complete form of the output signal from the Hall sensor is described by equation (2) as

$$U_\mathrm{out} = R_\mathrm{off}I + \frac{R_\mathrm{H}}{t}IB\mathrm{cos}(\alpha) + \frac{P_\mathrm{H}}{t}IB^2\mathrm{cos}(\beta)\mathrm{cos}(\gamma) \tag{2}$$

The desired signal U_H is only due to the second term on the right-hand side. It states that the Hall voltage U_H is directly proportional to the magnitude of measured magnetic field B. The other values are the biasing current I, the thickness of the conductive plate t and the Hall coefficient R_H. This number is specific to the material of the sample. For some materials, it is also a function of temperature T and the magnitude of measured magnetic field B [*Ďuran et al.*, 2017]. The factor cos(γ) represents the projection of the measured magnetic field **B** to the direction parallel with the normal to the sensor.

A more practical parameter of a Hall sensor related to its material is the Hall sensitivity S_H. It takes into account the normal Hall coefficient R_H and the sensor thickness t and provides information about the magnitude of the output signal given the biasing current and measured magnetic field as shown in equation (3)

$$S_{\mathrm{H}}(T, B) = \frac{R_{\mathrm{H}}(T, B)}{t} \qquad \left[\frac{\mathrm{V}}{\mathrm{A} \cdot \mathrm{T}}; \mathrm{m}^3 \cdot \mathrm{C}^{-1}, \mathrm{m}\right]. \tag{3}$$

Complementary to the normal Hall effect the planar Hall effect occurs as well. It is described by the third term on the right-hand side of 2. As the name suggests it is sensitive to the projection into the plane parallel to the surface of the sensors. This is accounted for by the factor cos(α)cos(β). The coefficient specific to this effect is the planar Hall coefficient P_{H} which is different from the normal Hall coefficient.

The first term on the right-hand side of 2 is the offset voltage. It can be observed when the Hall sensor is biased by current I but no magnetic field **B** is applied. This effect occurs due to a mismatch of the longitudinal and transverse resistances R_{off} of the Hall sensor. The mismatch is usually caused by manufacturing errors.

Spinning current method

The planar Hall voltage and the offset voltage are, for the sake of measuring the magnitude of the magnetic field, considered to be error voltages. To suppress those the spinning current method is employed. In this method, the sensing and biasing leads of a Hall sensor are periodically swapped. In other words, the Hall sensor is rotated by 90° periodically. Combined with the fact that the direction of the normal Hall voltage changes with a different period compared to the direction of the offset voltage and planar Hall voltage, averaging the output signals from individual commutations isolates the normal Hall voltage. A more detailed explanation of the application can be found in *Entler et al.* [2017b,c].

Hall sensors for fusion reactors

The commercially available Hall sensors are usually made with a semiconductor sensing layer which generally possesses a good sensitivity to magnetic field However, these off-the-shelf sensors tend to have low maximum operating temperatures (≈150 °C) as well as low resistance to radiation [*Ďuran et al.*, 2006]. This renders the semiconductor Hall sensors unsuitable for use in environments of fusion reactors.

At the Institute of Plasma Physics of the Czech Academy of Sciences (IPP CAS) in Prague Hall sensors based on ceramics and metals are developed to overcome the shortcomings of commercially available Hall sensors in terms of temperature stability and radiation resistance. An example of a Hall sensor with an antimony sensing layer is in Figure 1(right).

Sensors with metallic sensitive layers generally reach greater maximum operating temperatures, however, these sensors have sensitivities much lower compared to those with semiconductor layers [*Entler et al.*, 2021a].

The issue of radiation resistance of metallic Hall sensors has been investigated in *Ďuran et al.* [2017]; *Entler et al.* [2019, 2021a]. In the case of bismuth [*Ďuran et al.*, 2017] and antimony [*Entler et al.*, 2023] irradiation experiments were performed. It was concluded that both bismuth and antimony are to be used as steady-state magnetic diagnostics in ITER [*Entler et al.*, 2018, 2021b].

A simulation of transmutation of multiple candidate Hall sensor materials was performed [*Kovařík et al.*, 2020]. The simulation was made to mimic the conditions of DEMO Phase 1. That is a total fluence 6.08×10^{25} n/cm^2 in 5.2 years of operation. In the case of antimony the transmuted fraction of sensing material is predicted to be about 3.3 %. As another candidate for Hall sensor sensing material chromium was considered [*Entler et al.*, 2021a]. The result of the transmutation simulation for chromium show that the transmuted fraction in the case of chromium is only about 0.27 %.

Synchronous detection

Since metallic Hall sensors display relatively low sensitivity to magnetic field, the amplitude of their output signal is also relatively low: ≈ 150µV/T [*Entler et al.*, 2017a]. Signals of such low levels require careful signal conditioning as they may not be detectable due to the presence of noise. A method employed to overcome this problem is the synchronous detection. This method used to this day in broadcasting, can detect low-level signals and suppress noise. A schematic of an analog implementation of synchronous detection is shown in Figure 2(left).

The principle of this method is that a Hall sensor is biased by an alternating current with frequency f, as show in equation (4):

$$U_H(t) = S_{\mathrm{H}} B I \sin(2\pi f t), \tag{4}$$

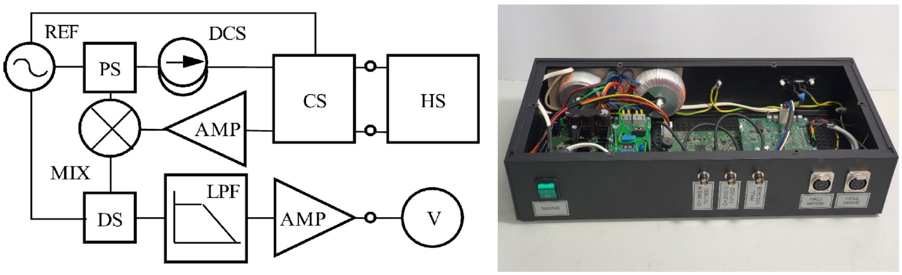

Figure 2. Scheme of an analog implementation of signal conditioning used with metallic Hall sensors developed at IPP CAS (left). Available from *Entler et al.* [2017c]. Photo of a digital Hall sensor controller developed at IPP based on the analog scheme (right).

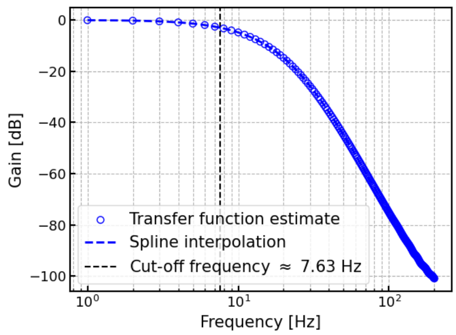

Figure 3. Simulated response function of the digital controller designed at IPP.

where S_H is the sensor's sensitivity, B is the magnitude of the measured magnetic field, I is the amplitude of the biasing current and f is the modulation frequency. In a mixer, the output signal is multiplied by that same sine wave that excites the Hall sensor. The result of the multiplication of two sine waves with generally different frequencies is given by equation (5) to be

$$A_1 \sin(2\pi f_1 t) \cdot A_2 \sin(2\pi f_2 t) = \frac{A_1 A_2}{2} \Big[\cos\big(2\pi(f_2 - f_1)t\big) - \cos\big(2\pi(f_2 + f_1)t\big)\Big]. \tag{5}$$

The output signal is excited and then multiplied by a reference $U_r = A\sin(2\pi f t)$ with the same frequency, that is $f = f_1 = f_2$ and subsequently a narrow low-pass filter is then applied to it. If the modulating frequency f is high enough the only remaining term is $A_1 A_2/2$ which corresponds to the only product of amplitudes of the original sine waves. This is described by equation (6)

$$m = S_{\mathrm{H}} I B A, \tag{6}$$

which is the normal Hall voltage multiplied by the amplitude of the modulation.

Hall sensor control electronics

A controller was developed at IPP to perform the synchronous detection and the spinning current method automatically. A detailed description of the algorithm used by the controller to employ both of these methods can be found in *Entler et al.* [2017a].

Recently a digital version of Hall sensor control electronics was developed. An image of the digital controller is shown in Figure 2(right). It is programmable and able to supply the connected Hall sensor with 1–10 mA of current. The modulation frequency of the controller is 5 kHz its sampling frequency is 256 kHz. The signal conditioning after digitization of the Hall sensor output includes a moving average with a window of 256 samples and 2 FIR low-pass filters of 3$^{\mathrm{rd}}$ order.

A simulation of the frequency response of the digital controller was done. The results of said simulation can be seen in Figure 3. As can be seen, the cut-off frequency of the controller was estimated to be around 7.6 Hz. Metallic Hall sensors that require extensive signal conditioning are thus viable only as steady-state magnetic field sensors.

Data fusion

Inductive sensors perform better when measuring magnetic fields with higher frequencies. While metallic Hall sensors suitable for fusion reactor-like environments perform well in lower frequencies due to their signal conditioning.

In this section an algorithm is proposed to combine the signals from an inductive and Hall sensor such that the drawbacks of the individual sensors are mitigated resulting in an estimate of the measure magnetic field that improves on the accuracy of each individual sensor.

The topic of applying data fusion to inductive and Hall sensors was explored in *Quercia et al.* [2022]; *Arpaia et al.* [2022]. In the former an algorithm named Luenberger observer was investigated. The latter employed Kalman filtering to combined the two sensor types. In this contribution the Kalman filter approach is described.

Data fusion of inductive and Hall sensors

Given that the magnetic diagnostic system including an inductive sensor and a Hall sensor can be considered a linear time-varying system [*Quercia et al.*, 2022], then the algorithm for combining those two sensors is described by equations (7) [*Arpaia et al.*, 2022] as

$$\begin{aligned}\hat{B}^{-}(k) &= \hat{B}^{+}(k-1) + \frac{T_{\mathrm{s}}}{2A_{\mathrm{c}}}(U_{\mathrm{c}}(k) + U_{\mathrm{c}}(k-1)) \\ \hat{P}^{-}(k) &= \hat{P}^{+}(k-1) + \sigma_{\mathrm{w}}^{2}(k) \\ K(k) &= \frac{\hat{P}^{-}(k)}{\sigma_{\mathrm{q}}^{2}(k) + \hat{P}^{-}(k)} \\ \hat{B}^{+}(k) &= \hat{B}^{-}(k) + K(k)\cdot(B_H(k) - \hat{B}^{-}(k)) \\ \hat{P}^{+}(k) &= (1 - K(k))\cdot\hat{P}^{-}(k).\end{aligned} \tag{7}$$

where T_s is the sampling time of the inductive sensor, A_c is its effective area, $U_c(k)$ is the signal from the inductive sensor at time k, $\sigma_q(k) = 1$ mT is the variance of the Hall sensor, $B_H(k)$ is magnetic field measured by the Hall sensor and $\sigma_w^2(k)$ is the variance of the integral increment computed from the inductive sensor signal given by equation (8)

$$\sigma_{\mathrm{w}}^{2}(k) = \frac{T_{\mathrm{s}}^{2}}{4A_{\mathrm{c}}^{2}}\left(\frac{\sigma_A^2}{A_{\mathrm{c}}^2}(U_{\mathrm{c}}(k) + U_{\mathrm{c}}(k-1))^2 + (\sigma_U^2(k) + \sigma_U^2(k-1))\right), \tag{8}$$

where $\sigma_U(k) = 1$ mV and $\sigma_A = 3.8\cdot 10^{-2}$ cm^2. These were estimated based on the information provided by *Quercia et al.* [2022].

The symbols $\hat{B}$ and $\hat{P}$ denote the magnetic field estimate and the estimate of the variance of the magnetic field estimate. The super-indexes $^-$ and $^+$ denote the prediction and correction respectively. The value $K(k)$ is called Kalman gain and is a comparison between the predicted variance of the estimate and the variance of the Hall sensor. It is a number between 0 and 1 and determines which of the two sensors is more trustworthy at any given time k.

Note that the algorithm operates with only the information about the current and previous time step which makes it suitable for real time application.

Data fusion application

To show the performance of the Kalman filter data from the JET tokamak were analysed. The tokamak discharge in question was numbered 94818. During the discharge radial magnetic field was measured at the lower part of the vacuum vessel (see Figure 4left) by both a coil and a Hall sensor (see Figure 4right). The output signal of the Hall sensor is shown in Figure 5(left) and of the coil in Figure 5(right). After applying the Kalman filter algorithm described by equation (7) the resulting magnetic field estimate is shown in Figure 6(left). In Figure 6(right) a comparison is made between the Kalman filter output and the magnetic field calculated as an integral of the signal from the coil with the offset removed. As can be seen from Figure 6 the proposed algorithm is able to suppress the noise of the Hall sensor as well as mitigate the drift of the integrated signal from the inductive sensor.

Conclusion

Tokamaks are devices designed to contain hot plasma using magnetic fields. Thus, it is crucial to measure the tokamak magnetic field during discharges accurately. A common method of tokamak magnetic diagnostics is utilising inductive sensors. While performing well in high frequencies they lack sensitivity for low-frequency fields and are prone to low-frequency error voltages. As a complement to inductive sensors metallic Hall sensors are being developed at IPP CAS.

The focal points of research and development of metallic Hall sensors are their temperature stability and their radiation resistance. In recent years bismuth and antimony Hall sensors were confirmed to be suitable for operation in ITER-like conditions. In further research, the feasibility of using antimony Hall sensors in DEMO-like conditions will be investigated. A simulation was performed and it was concluded that chromium Hall sensors can function in DEMO-like conditions as well, though their sensitivity is much lower than that of antimony Hall sensors.

A potential for data fusion of inductive and Hall sensors is being investigated. For that purpose, the Kalman

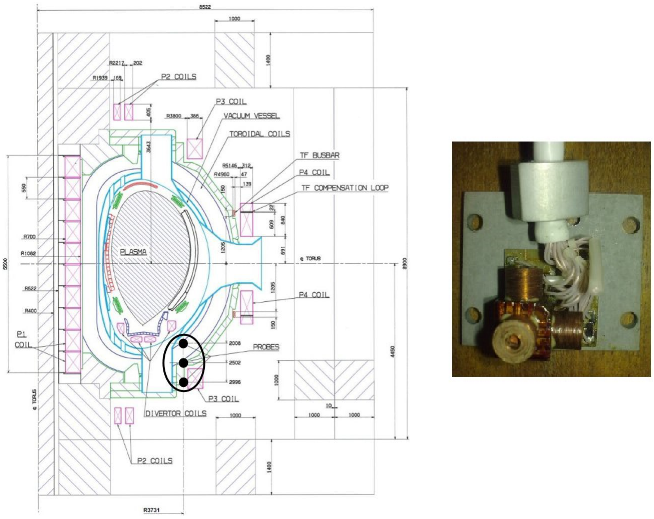

Figure 4. Placement of the Hall sensors and pick-up coils on the JET machine (left). Combined probe from Hall and inductive sensor used at JET to measure magnetic field. Available from *Quercia et al.* [2022]

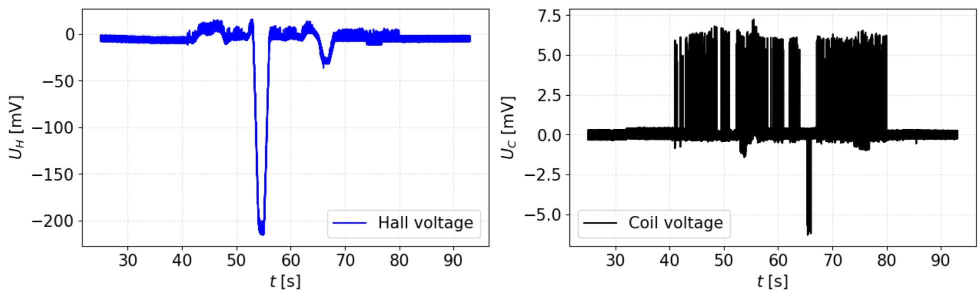

Figure 5. Output signals from Hall sensor (left) and pick-up coil (right) from JET discharge number 94818. Measurement of radial magnetic field in the lower part of vacuum vessel.

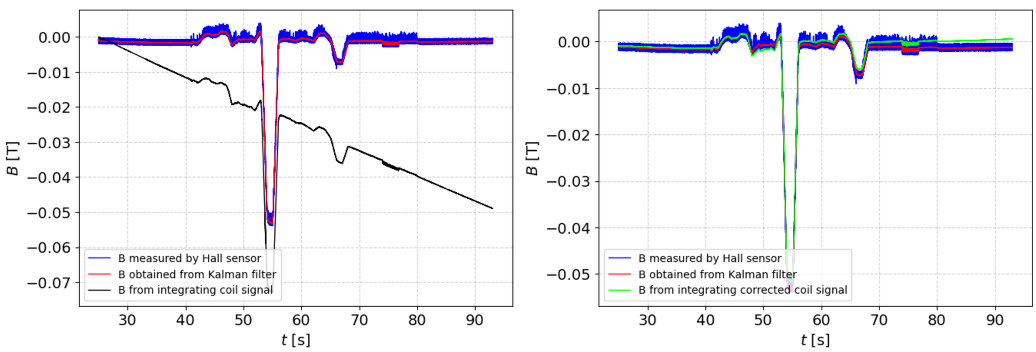

Figure 6. Result of applying the Kalman filter algorithm (red) on the signals from the Hall sensor (blue) and the pick-up coil (black). Left, comparison of Kalman filter to the integral of the corrected coil signal (lime) is made.

filter algorithm is being explored and it was shown that it can compensate for the shortcomings of the individual sensors. In further research, a continuous refinement of the Kalman filter algorithm is planned as well as an employment of an explicit dependence of the algorithm on the frequency of the measured signals.

References

Arpaia, Pasquale; Buzio, Marco; Di Capua, Vincenzo; Grassini, Sabrina; Parvis, Marco et al. Drift-Free Integration in Inductive Magnetic Field Measurements Achieved by Kalman Filtering. Online. Sensors. 2022, 22, 1. ISSN 1424–8220. Available from: https://doi.org/10.3390/s22010182.

Batista, Antonio J.N.; Naylor, Graham; Capellà, Llorenç; Neto, Andre; Stephen, Adam et al. Testing results of chopper based integrator prototypes for the ITER magnetics. Online. Fusion Engineering and Design. 2018, 128, pp. 193–197. ISSN 09203796. Available from: https://doi.org/10.1016/j.fusengdes.2018.01.065.

Ďuran, Ivan; Entler, Slavomír; Kočan, Martin; Kohout, Michal; Viererbl, Ladislav et al. Development of Bismuth Hall sensors for ITER steady state magnetic diagnostics. Online. Fusion Engineering and Design. 2017, 123, pp. 690–694. ISSN 09203796. Available from: https://doi.org/10.1016/j.fusengdes.2017.05.142

Ďuran, I.; Viererbl, L.; Klupák, V.; Bolshakova, I.; Holyaka, R. Investigation of stability of ITER candidate Hall sensors under neutron irradiation. Online. Czechoslovak Journal of Physics. 2006, 56, S2, pp. B54–B60. ISSN 0011-4626. Available from: https://doi.org/10.1007/s10582-006-0177-4.

Entler, S.; Duran, I.; Sladek, P.; Vayakis, G.; Kočan, M. Signal conditioning and processing for metallic Hall sensors. Online. Fusion Engineering and Design. 2017, 123, pp. 783–786. ISSN 09203796. Available from: https://doi.org/10.1016/j.fusengdes.2017.04.106.

Entler, S. and Ďuran I. Kovové Hallovy senzory. Československý časopis pro fyziku [online]. 2017, 91–101. Available from: http://www.ipp.cas.cz/miranda2/export/sitesavcr/ufp/ufp-v-mediich/Publications/Kovove-Hallovy-senzory.pdf

Entler, S.; Duran, I.; Sladek, P.; Vayakis, G.; Kočan, M. Signal conditioning and processing for metallic Hall sensors. Online. Fusion Engineering and Design. 2017, 123, pp. 783–786. ISSN 09203796. Available from: https://doi.org/10.1016/j.fusengdes.2017.04.106.

Entler, S.; Duran, I.; Kocan, M.; Vayakis, G.; Kohout, M. et al. Prospects for the steady-state magnetic diagnostic based on antimony Hall sensors for future fusion power reactors. Online. Fusion Engineering and Design. 2019, 146, pp. 526–530. ISSN 09203796. Available from: https://doi.org/10.1016/j.fusengdes.2019.01.013.

Entler, Slavomir; Duran, Ivan; Kocan, Martin; Vayakis, George; Sladek, Petr et al. Calibration of the ITER outer vessel steady-state magnetic sensors. Online. Fusion Engineering and Design. 2021, 168. ISSN 09203796. Available from: https://doi.org/10.1016/j.fusengdes.2021.112398.

Entler, S.; Duran, I.; Simonovsky, M.; Reboun, J.; Turjanica, P. et al. Antimony Hall sensor testing at ITER and DEMO relevant temperatures. Online. Fusion Engineering and Design. 2023, 189. ISSN 09203796. Available from: https://doi.org/10.1016/j.fusengdes.2023.113476.

Entler, S.; Sebek, J.; Duran, I.; Vyborny, K.; Grover, O. et al. High magnetic field test of the ITER outer vessel steady-state magnetic field Hall sensors at ITER relevant temperature. Online. Review of Scientific Instruments. 2018, 89, 10. ISSN 0034-6748. Available from: https://doi.org/10.1063/1.5038812.

Entler, Slavomir; Soban, Zbynek; Duran, Ivan; Kovarik, Karel; Vyborny, Karel et al. Ceramic–Chromium Hall Sensors for Environments with High Temperatures and Neutron Radiation. Online. Sensors. 2021, 21, 3. ISSN 1424–8220. Available from: https://doi.org/10.3390/s21030721.

Kovarik, Karel; Entler, Slavomir; Duran, Ivan; Eade, Tim. Analysis of Transmutation of Candidate Sensitive Layer Materials of Hall Detectors under DEMO Like Neutron Fluxes. Online. Fusion Engineering and Design. 2020, 155. ISSN 09203796. Available from: https://doi.org/10.1016/j.fusengdes.2020.111670.

Quercia, A.; Pironti, A.; Bolshakova, I.; Holyaka, R.; Duran, I. et al. Long term operation of the radiation-hard Hall probes system and the path toward a high performance hybrid magnetic field sensor. Online. Nuclear Fusion. 2022, 62, 10. ISSN 0029-5515. Available from: https://doi.org/10.1088/1741-4326/ac8aad.